33RD CONGRESS
OF THE INTERNATIONAL COUNCIL
OF THE AERONAUTICAL SCIENCES
STOCKHOLM, SWEDEN, 4–9 SEPTEMBER, 2022

ICAS 2022 SWEDEN

DOPAMINE-COATED UHMWPE/HYDROGEN-RICH BENZOXAZINE COMPOSITES FOR SPACE RADIATION SHIELDING

Ji-Hun Cha[1] and Chun-Gon Kim[*1]

[1]Department of Aerospace Engineering, KAIST, 291, Daehak-ro, Yuseong-gu, Daejeon, Republic of Korea

First author. E-mail: jihundd@kaist.ac.kr

*Corresponding author. E-mail: cgkim@kaist.edu

Phone: +81-42-350-3719; fax: +82-10-350-3710; http://smartech.kaist.ac.kr

Abstract

Recently, COTS (commercial off-the-shelf) is being used as an electronic device for high performance and low cost of satellites. However, COTS is vulnerable to cosmic radiation. UHMWPE/hydrogen-rich benzoxazine composite (UHC) has excellent cosmic radiation shielding performance. However, the low interfacial adhesion of UHMWPE fibers causes the low flexural strength and delamination of UHC. It was possible to increase the interlaminar shear strength of UHC by polydopamine coating, MWCNT and amine grafting on UHMWPE. The space environment resistance was tested on UHC, and the cosmic radiation shielding performance was compared with existing space materials.

Keywords: UHMWPE, hydrogen-rich benzoxazine, dopamine coating, interlaminar shear strength, cosmic radiation

1. Nomenclature

COTS = commercial off-the-shelf
LEO = low earth orbit
UHMWPE = ultra-high-molecular-weight polyethylene fiber
HRB = hydrogen-rich benzoxazine
UHC = UHMWPE fiber and hydrogen-rich benzoxazine matrix composite
PDA = polydopamine
OLTARIS = cosmic radiation analysis tool available on the online
PE = polyethylene
SEM = scanning electron microscope
CVCM = collected volatile condensable materials
TML = total mass loss
FTIR = fourier transform infrared spectroscopy
XPS = X-ray photoelectron spectroscopy

2. Introduction

The space industry, which started as a result of competition between the United States and the Soviet Union during the Cold War, has passed the era of government-led space competition and military development, and is entering the era of private companies-led New Space. In particular, startups of

various sizes are emerging to development and utilization of small satellites (or CubeSat) among the satellite applications where private participation have been active. Small satellites have been attracting great attention from universities, and private companies, and state-owned because they can significantly reduce development costs and time compared to medium and large satellites.

Recently, private small satellite development companies have been using COTS (commercial off-the-shelf) as their satellite electronics for high performance and low development cost. However, compared to space-only electronic equipment, COTS is particularly vulnerable to cosmic radiation (galactic cosmic ray, solar energetic particle, and trapped proton)[1]. Therefore, early retirement and some failure problems in small satellites that actively use COTS can be caused by cosmic radiation problems (total ionizing dose, single event effect, and displacement damage)[2]. In fact, About half of the small satellites that failed from 2009 to 2018 were caused by malfunctions in electronics[3], and some are suspected to be caused by cosmic radiation[4]. In addition, the lifespan of COTS is generally limited to around 1 year at low Earth orbit (LEO)[5]. Therefore, increasing the cosmic radiation shielding performance of small satellites can reduce failures, increase reliability and extend the mission period.

According to the Bethe-Bloch formula, an element with a high Z (number of electrons) / A (relative atomic mass) is effective in reducing the radiation dose by reducing the kinetic energy of protons and heavy ions[6], which are the main elements of cosmic radiation, and reduces the generation of secondary radiation[7][8]. Hydrogen, the element with the highest Z / A, is the most effective element for cosmic radiation shielding. Therefore, materials containing lots of hydrogen elements have been proposed as cosmic radiation shielding materials[9]. We noted that hydrogen-rich benzoxazine (HRB) developed by Iguchi et al.[10] has more hydrogen than any other thermosetting resin (epoxy, etc.). HRB has the following characteristics; in general, the molecular structure of ultra-high-molecular-weight polyethylene (UHMWPE) is known to degrade gradually from 130°C, so HRB is designed to polymerize and crosslink at 120°C for UHMWPE fiber reinforced composite applications[11]; HRB has many advantages for space structure applications because it has high thermal stability, low coefficient of thermal expansion, high mechanical properties, excellent chemical resistance, and a long storage period[10][11][12].

UHMWPE fiber has superior radiation shielding performance, high tensile properties, low density, high impact strength, and space environment resistance, so it is highly anticipated for future space structure applications[13][14][15]. One of the important limitations in the application of UHMWPE fiber-reinforced composites to satellite structures is the low interfacial adhesion of UHMWPE fiber. UHMWPE fiber lacks polar functional groups and has a low surface free energy, so the adhesion between the UHMWPE fiber and the matrix is very poor[16]. Although the tensile properties of UHMWPE fiber reinforced composites are excellent, the low interfacial adhesion of UHMWPE fibers lowers the compressive strength, bending strength, buckling load, and interlaminar shear strength of UHMWPE fiber reinforced composites, and in severe cases may cause delamination[17]. Therefore, in order to increase the interfacial adhesion of UHMWPE fiber, studies such as potassium permanganate treatment[18], poly pyrrole coating[17], dopamine coating, plasma treatment[19], UV-irradiation[20], glycidyl methacrylate grafting and nano-reinforcement[21][22], etc. have been performed. However, with the exception of only a few studies on fiber coatings such as poly dopamine (PDA) coating, most of the reported interfacial property improvement studies have been found to damage the fibers and sacrifice their tensile properties[23]. Assuming that UHMWPE fiber-reinforced composite is used as a satellite structural panel, tensile stiffness cannot be given up to withstand the launch load and vibration[24]. In addition, the simplicity of manufacture and the possibility of mass production must be considered in the work to improve the interfacial adhesion of UHMWPE fiber. Therefore, this study focused on UHMWPE fiber-reinforced composite based on PDA coating was studied in consideration of the preservation of tensile strength, cost efficiency, and practical applicability among methods to improve the interfacial adhesion of fibers[23].

In outer space, due to ultra-high vacuum and high temperature, the polymer materials of spacecraft emit gases and decomposed fine particles can stick to the electronic equipment of the satellite, deteriorating performance or in severe cases. Due to the ultra-high vacuum and high temperature in outer space, the polymer materials of spacecraft generate volatile gases or fine particles by outgassing, which can stick to satellite electronic equipment, deteriorating performance, or in severe

cases, failure. In addition, total mass loss (TML) of polymer materials due to outgassing can cause mechanical properties to decrease. Therefore, according to Space Heritage, traditional spacecraft materials must meet collected volatile condensable materials (CVCM) <0.1% and TML <1.0%[14]. However, since CVCM and TML data for UHMWPE/HRB composite (UHC) have not yet been reported, the CVCM and TML tests for UHC were first performed in this study

The purpose of this project can be summarized as follows: to maximize the interlaminar shear strength (ILSS) without sacrificing the tensile properties of UHMWPE fiber, we develop UHC with PDA coating, hexamethylene diamine (HMDA) grafting and functionalized MWCNT applied; In the LEO space environment where the heat flux is considered, it is to evaluate how much the mechanical properties of the proposed composite material have decreased under MLI protection; and we analyze how much UHC can reduce the radiation dose of LEO compared to existing space materials. The final goal of this study is to show that the proposed composite material can be applied as a structural panel for small satellites.

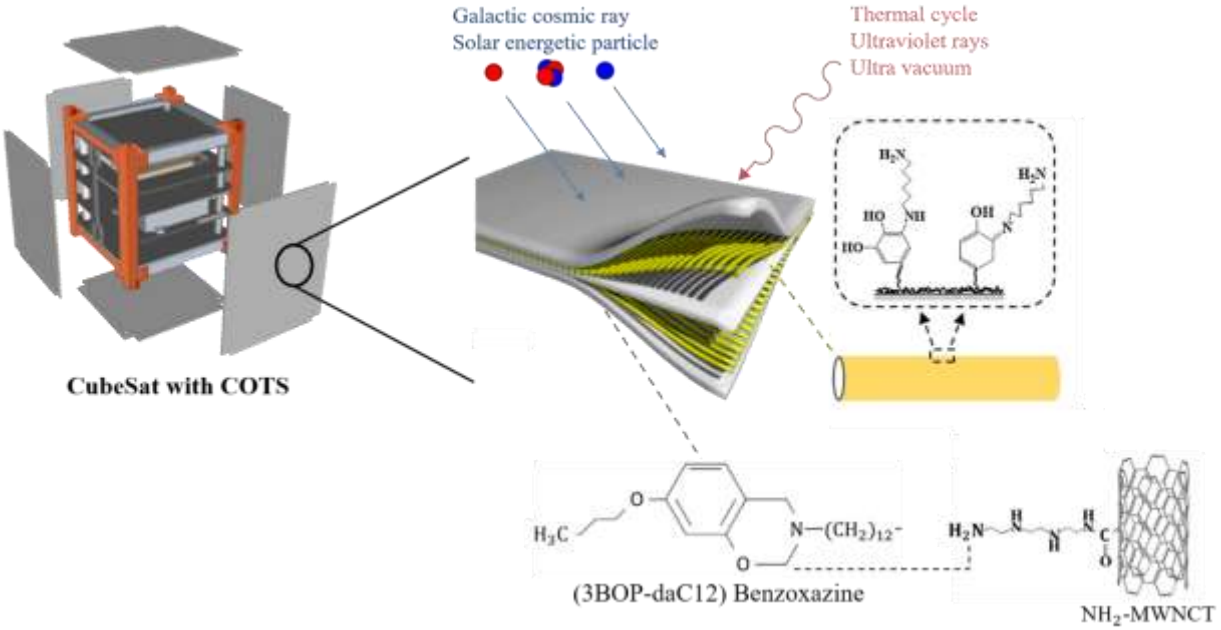

Figure 1 – Research schematic.

3. Methodology

3.1 Materials

SK99 (880 decitex, 800 denier), a UHMWPE fiber supplied from DSM Dyneema, was used. As far as we know, SK99 is the UHMWPE fiber with the highest tensile performance. SK99 fibers were woven into plain weave (173 g/m2) by HWASUNG International CO. 3-butoxyphenol, 1,12-diaminododecane, and sodium hydroxide were purchased from Tokyo Chemical Industry. Chloroform and anhydrous magnesium sulfate were purchased from Alfa Aesar. Paraformaldehyde, dopamine hydrochloride, tris base, and hexamethylenediamine (HMDA) were purchased from Sigma-Aldrich.

Referring to Zeng et al. [29], which investigated the aspect ratio of MWCNT, which can increase the bonding strength between the fiber and the matrix, COOH-MWCNT (carboxylic acid functionalized) and NH2-MWCNT (amino functionalized) with a outer diameter of 10-20 nm and a length of 10-30 μm were selected; Purchased from US Research Nanomaterials.

3.2 Hydrogen-rich benzoxazine (HRB) manufacturing processes

Although HRB production was attempted by referring to Iguchi et al.[10], we had many failures in the production of HRB, and detailed production methods learned through numerous trials and errors in the production process are as follows. 3-butoxyphenol, 1,12-diaminododecane, and paraformaldehyde were mixed with mole ratio = 2: 1: 4.2, chloroform (5 mL/g of reactants) and heated and stirred until a little bubble appeared; Normally, the beaker was heated with 57℃ heating water

with 600 RPM magnetic stirring for 5 hours. After that, when the temperature of the reaction product was sufficiently low, neutralization was performed with Sodium Hydroxide (1mol/L in water) and DI water; At this time, the neutralization solution was separated from the reaction product using a chromatography column. Then, while cooling the beaker of the reaction product with cold water, anhydrous magnesium sulfate equivalent to about 1/4 of the weight of the reaction product was added to the reaction product and dehydrated for about half a day. Anhydrous magnesium sulfate was completely filtered from the reaction product using a vacuum filter with a minimum pore size of 3 μm; As the reaction product passed through the vacuum filter, most of the moisture (chloroform and neutralizing solution) was removed, so the filtered reaction product was directly used in the hand lay-up process.

Table 1 – Converting mole fraction to mass for HRB production.

	3-Butoxyphenol $C_{10}H_{14}O_2$ **(1g to 0.006016 mol)**	**1,12-diaminododecane** $C_{12}H_{28}N_2$ **(1g to 0.004991 mol)**	**Paraformaldehyde** $OH(CH_2O)_nH$ **(1g to 0.033300 mol)**	**Chloroform** $CHCl_3$ **(1g to 0.008377 mol)**
Synthesis rate: 2 : 1 : 4.2 (mol) + Chloroform (5 mL/g of reactants)	10.000 g (0.060161 mol)	6.027 g (0.030081 mol)	3.794 g (0.126339 mol)	147.866 g (1.238616 mol)

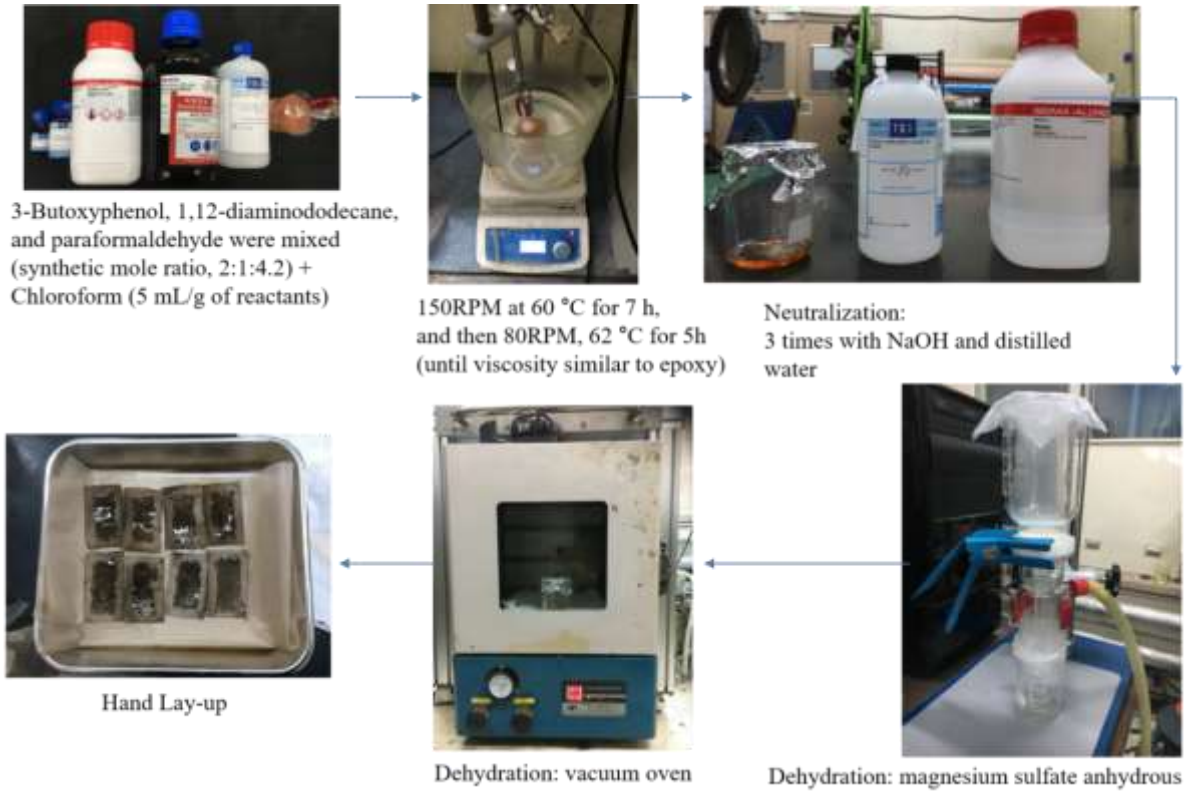

Figure 2 – Hydrogen-rich benzoxazines production process.

3.3 Dose analysis of UHMWPE / HRB composite in LEO

To verify how much UHC or HRB-applied satellites can reduce low-Earth orbit doses compared to conventional space materials, annual cosmic radiation doses were calculated using OLTARIS[35]. The elemental composition in Table 1 and orbital information (500km, 97.5°) of the KARI HiReV cube satellite were used for OLTARIS analysis. In addition, as the GCR model and the trapped model, Badhwar-O'Neil 2020 and AP9 were used to analyze the dose. Considering the maximum panel thickness applicable to a typical satellite, the annual dose (Gy/year) at an areal density of 0.5 g/cm^2 and 1 g/cm^2 was compared with other space materials.

3.4 Modification of UHMWPE fibers

UHMWPE plain woven fabric was washed ultrasonically for 30 minutes using DI water, and repeated three times. After that, UHMWPE was put in a vacuum chamber at 50℃ for 8 hours and used in a completely dried and clean state.

UHMWPE coated with PDA (PDA-UHMWPE): 1) Dopamine hydrochloride was added at 2 g / L in DI water, and tris base (usually 1.2 g / L) was added to adjust the pH value to 8.5; 2) The cleaned UHMWPE fibers were immersed in a dopamine solution for 24 hours at room temperature, followed by magnetic stirring; 3) It was rinsed several times with DI water and vacuum dried at 40℃ for 6 hours.

UHMWPE coated with PDA and MWCNT (PDA-MWCNT-UHMWPE): 0.01wt% (or 0.03wt etc.) of MWCNT was added to DI water and sufficiently dispersed with a sonicator[30]; The rest of the process is made the same as 1), 2) and 3) of PDA-UHMWPE.

HMDA grafting in PDA-MWCNT-UHMWPE (PDA-MWCNT-HMDA-UHMWPE): 1) After adjusting the pH to 8.5 with hydrochloric acid in 10 mM Tris buffer, PDA-MWCNT-UHMWPE was immersed; 2) Into DI water equivalent to 1/9 of the volume of the previous buffer, 1 g/ml of HMDA was added, slowly added to the buffer, and magnetic stirring was performed for 8 hours[31]; 3) It was rinsed several times with DI water and vacuum dried at 40℃ for 6 hours.

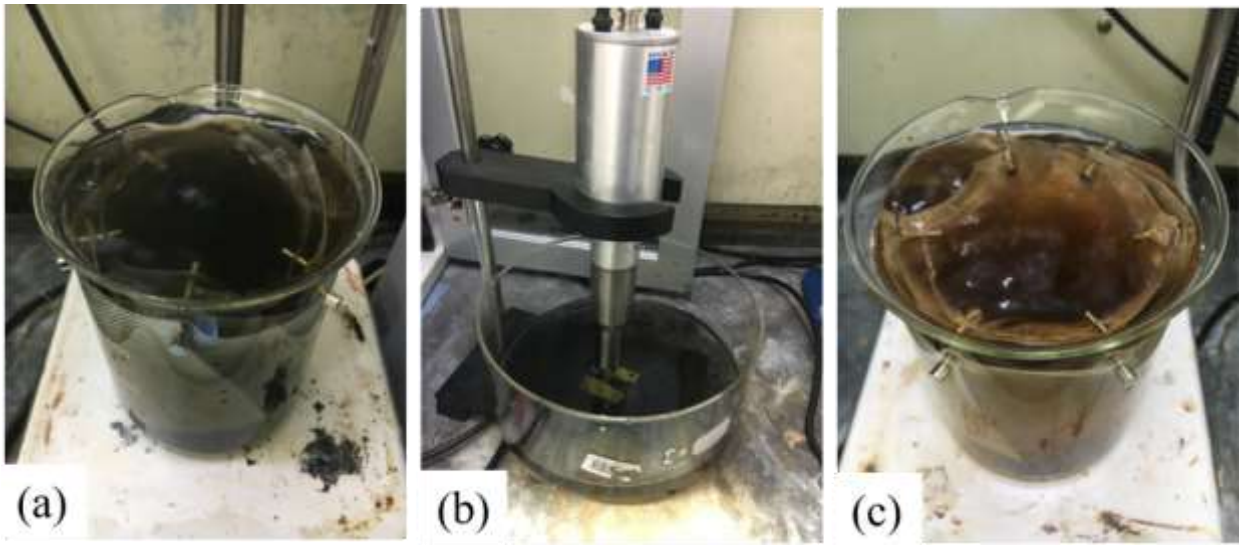

Figure 3 – Fiber coating and grafting; (a) PDA coating; (b) PDA coating and MWCNT grafting; (c) Hexamethylenediamine grafting.

3.5 UHMWPE / HRB composite (UHC) manufacturing processes

In the previous study[11], UHC was produced by vacuum packaging process with little pressure, but in this study, the following sequence of processes was introduced to maximize the interlaminar shear strength of UHC; 1) HRB was Hand lay-up on PDA-based coated UHMWPE plain woven fabric using a silicone spatula; 2) It was put in a vacuum chamber at room temperature for about 2 hours to completely remove air bubbles and moisture from the HRB; 3) After laminating the resin sides to each other, repeat 1) and 2) to stack the desired number; 4) Laminated plain woven fabric were produced with high pressure composite autoclave; Laminated plain woven fabrics were vacuum maintained and cured with the temperature cycle of the previous study[11] at a pressure of 4 bar; According to Lee et al. [32], the PDA was confirmed to be sufficiently stable even at 120℃ by thermogravimetric analysis, so the PDA coating does not decompose in a curing cycle of 120℃.

The reason for this manufacturing processes is that when curing begins and the temperature of the HRB increases, the viscosity increases, making it difficult to completely remove moisture and air bubbles. On the other hand, if the HRB's moisture and air bubbles are completely removed and hand lay-up, the hand lay-up process becomes very difficult, and the high viscosity of the HRB may damage the fibers.

Figure 4 – Autoclave production process.

3.6 Mechanical experiment

ILSS experiments were performed according to ASTM D2344M-16, and ILSS specimens were manufactured with a thickness of about 5.9-6.1 mm by stacking 24 fabric of ILSS specimens.

To examine the difference in tensile properties according to the fiber coating, a tensile test was performed according to ASTM D3039M-17. However, due to the low surface friction of UHC, the tensile specimen slipped from the wedge action grip. Therefore, referring to the previous study[34], a tensile test was performed using a hydraulic grip of 5 MPa. Tensile specimens were laminated to have a thickness of about 2.4-2.6mm.

To estimate the fiber volume fraction of the manufactured UHC, the HRB weight was calculated using the fabric weight and the weight of the UHC after fabrication, and the fiber volume fraction was calculated using the fiber density(0.97 g/cm^3) and the HRB density(1.07 g/cm^3).

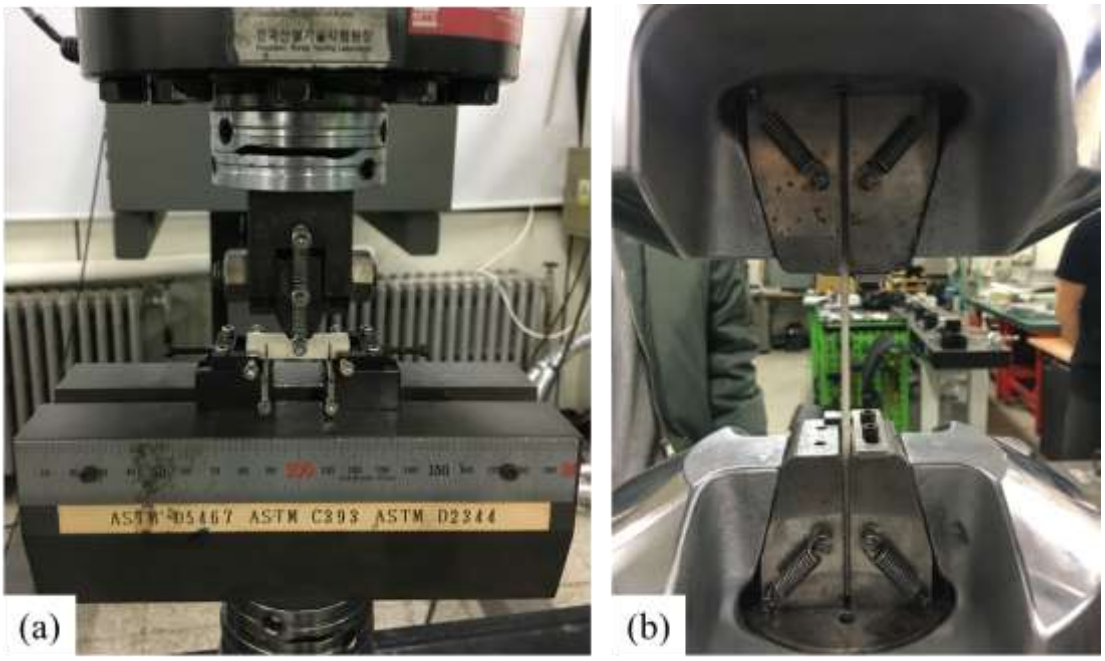

Figure 5 – (a) Interlaminar shear strength (ASTM-D2344M), (b) Tensile strength test (ASTM-3039M).

3.7 Modified fiber surface analysis

Surface chemical compositions for PDA coating, functionalized MWCNT and grafted HMDA groups were analyzed via X-ray photoelectron spectroscopy (XPS, Thermo VG Scientific) with Al Kα X-ray. A scanning electron microscope was used to observe the surface morphology of the modified UHMWPE. A scanning electron microscope (SEM, FEI Quattro S) at 2.5kV was used to observe the surface morphology of the fibers mentioned.

3.8 FTIR analysis of HRB according to curing temperature and time

Fourier transform infrared spectroscopy (FTIR) analysis of HRB was performed with a Nicolet iS50 FTIR Spectrometer to explain the difference in mechanical properties according to curing temperature and time in the final process. After spreading the HRB thinly on the silicone mold, the temperature was increased at 0.3℃/min in a vacuum chamber, and HRB cured at 120℃ - 2 hours and 130℃ - 10 hours in the final process was compared. The thickness of the fabricated HRB was 0.8-1 mm, and the data obtained through the attenuated total reflectance mode were compared in the paper. FTIR data obtained via the attenuated total reflectance mode were compared in this study.

3.9 Space environment experiment

As in the author's previous study[14], UHC's CVCM and TML experiments were performed with reference to ASTM E595-15. CVCM was measured using CVCM measuring dedicated equipment (Korea Research Institute of Standards and Science, Daejeon, Republic of Korea), and TML was measured using space environment simulation facility (Korea Advanced Institute of Science and Technology, Daejeon, Republic of Korea). CVCM and TML specimens were stacked with 18 layers and were performed with UHC with a thickness of 4.4-4.6mm and an area of 9×9mm and a mass of 0.3-0.4g.

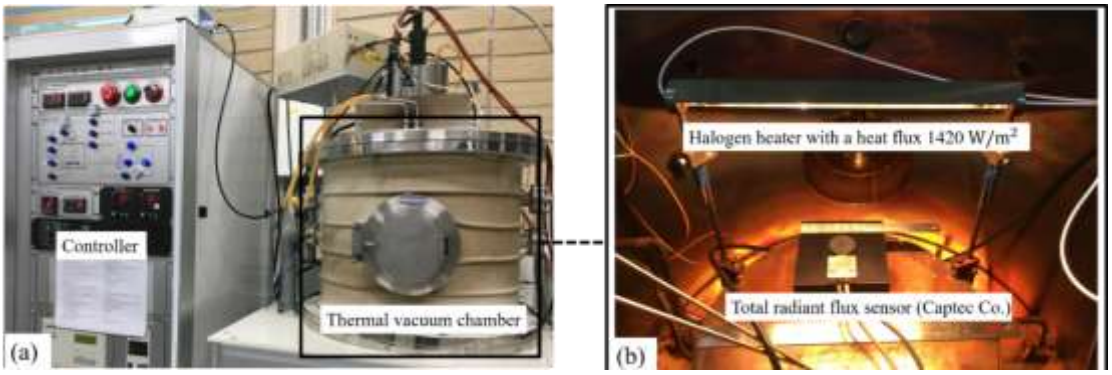

Figure 6 – Schematic diagram of space environment experiment; (a) TML test equipment, (b) inside the TML test equipment.

Figure 7 – Schematic diagram of space environment experiment; CVCM equipment.

4. Results and Discussion

4.1 Analysis of elemental content of HRB

The elemental content of HRB as measured by an organic element analyzer is shown in Table 2, and the elemental content is compared with the theoretical values of HRB and epoxy. Since the prepared HRB has a difference in element content of less than 0.16% between the theoretical value and the measured value, and was manufactured with the same reagent and molar fraction as in Iguchi et al.[10], it could be judged that the HRB produced in this study was made almost identical to the theoretical chemical structure. It was confirmed that HRB has about 11% higher hydrogen content than conventional aerospace epoxy (Cytec CYCOM 934). HRB, which has a higher hydrogen content than conventional thermosetting resins, has a positive effect on radiation shielding and shows better performance than epoxy in LEO dose analysis.

Table 2 – Comparison of the element content of HRB

Thermosetting resin (density)	Molecular formula	Composition		Difference between theoretical and measured values
		Theoretical value	Average of the measured values (Std. Dev.)	
HRB (1.07 g/cm^3)	$C_{36}H_{56}N_2O_4$ [10]	H = 57.1429% C = 36.7347% O = 4.0816% N = 2.0408%	H = 57.3002% (0.047) C = 36.5763% (0.204) O = 4.1036% (0.240) N = 2.0199% (0.016)	0.1573% 0.1584% 0.0220% 0.0209%
Epoxy (Cytec CYCOM 934) (1.32 g/cm^3)	$C_{37}H_{42}N_4O_6$ S [36]	H = 46.6667% C = 41.1111% O = 6.6667% N = 4.4444% S = 1.1111%		

4.2 Dose reduction performance of UHC and HRB in LEO

Fig. 8 shows the dose analysis results of OLTRAIS and Table shows the quantitative doses of 0.5 g/cm^2 and 1 g/cm^2. The smaller the areal density, the higher the dose reduction effect of hydrogen-rich materials than conventional materials. On the other hand, as the areal density increases, the dose reduction effect of many materials decreases compared to conventional materials, but the hydrogen-rich materials still guarantee a low radiation dose. At areal density of 0.5-1 g/cm^2, HRB can reduce the dose by about 3-4% more than the epoxy. In addition, UHC (60% fiber volume) can reduce dose by about 7-10% compared to CFRP (60% fiber volume) and about 21-28% compared to aluminum. UHC has less than 1% difference in shielding performance from UHMWPE, so UHC has almost the same radiation shielding performance as UHMWPE.

The dose reduction effect is as follows when explaining the TID (total ionizing dose) limit dose and lifetime of COTS. Assume that the TID limit for COTS is the dose protected by CFRP for one year

(1.307 Gy). If replaced with UHC of the same areal density, the lifespan of COTS can be increased by about 1-2 months. In addition, when replaced with UHC having double areal density (1 $\mathrm{g/cm^2}$), an increase in lifespan of about 6-7 months can be expected. Therefore, the structural performance of spacecraft can be dramatically improved by replacing the radiation shielding polyethylene with UHC, or the radiation shielding weight can be reduced or the radiation dose can be reduced by replacing the existing space material with UHC.

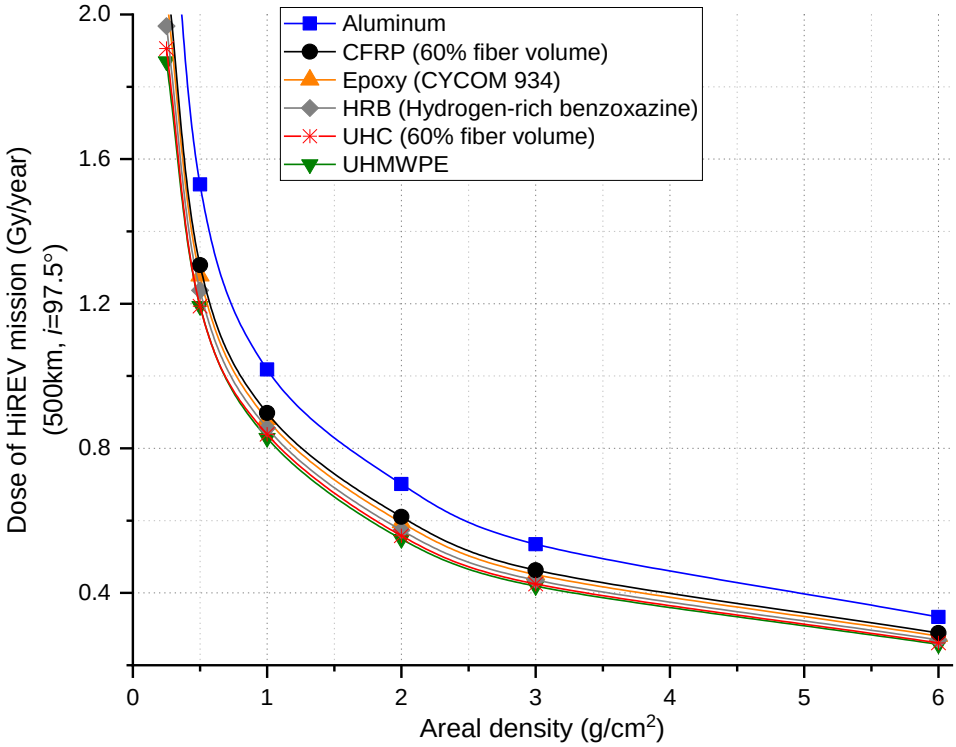

Figure 8 – Dose reduction effect of LEO satellite according to panel thickness and material.

Table 3 – Comparison of doses from LEO satellites with 0.5 $\mathrm{g/cm^2}$ and 1 $\mathrm{g/cm^2}$ panels in various materials.

	Aluminum	CFRP (60% fiber volume)	Epoxy	HRB	UHC (60% fiber volume)	UHMWPE
Annual dose at 0.5 $\mathrm{g/cm^2}$ (Gy/year)	1.530	1.307	1.277	1.237	1.193	1.190
(Comparison of dose to UHC)	(+28.2%)	(+9.6%)	(+7.0%)	(+3.7%)	-	(−0.3%)
Annual dose at 1 $\mathrm{g/cm^2}$ (Gy/year)	1.018	0.898	0.880	0.856	0.837	0.829

(Comparison of dose to UHC)	(+21.6%)	(+7.3%)	(+5.1%)	(+2.2%)	-	(−1.0%)

4.3 Interlaminar shear strength (ILSS)

In the autoclave process of UHC fabrication, the pressure affected the fiber volume fraction. The specimens made at 1 bar had a low fiber volume fraction (0.58-0.61), and the specimens made at 7 bar had a high fiber volume fraction (0.71-0.73). High fiber volume fractions have low ILSS performance, while low fiber volume fractions have low tensile properties with ILSS values similar to the intermediate fiber volume fractions. Therefore, in this study, in order to adjust the fiber volume fraction to 0.65 to 0.68, UHC specimens were prepared using a pressure of 4 bar in the autoclave process.

The ILSS test results of UHCs fabricated from UHMWPE with dopamine coating, functionalized MWCNT, and HMDA grafting are shown in Fig. 8, and ILSS specimens and test photos are shown in Fig. 9. In pristine UHMWPE, the ILSS could be increased by about 36% only by increasing the heating temperature and heating time of the final process. Although the tensile properties of UHMWPE can be degraded at 130°C long-term heating, 130°C heating showed higher ILSS performance than 120°C heating. Also, heating for 10 hours has mostly higher ILSS values than heating for 5 hours. On the other hand, there was no significant difference in ILSS values for 20 hours heating and 10 hours heating. Heating at 130°C for 20 hours can degrade the properties of the fiber, so a process of 10 hours at 130°C or 5 hours at 130°C is recommended. The PDA coating process was able to increase the ILSS by about 59% compared to the pristine process. PDA coating and functionalized MWCNT grafting was able to increase ILSS by approximately 113% over the pristine process. PDA coating and HMDA grafting were able to increase ILSS by about 131% over the pristine process. PDA coating, MWCNT and HMDA grafting were able to increase ILSS by about 162% compared to the pristine process. To increase the interfacial adhesion of UHMWPE-HRB, a complex coating-grafting process and temperature conditions for higher curing were added, but the ILSS value was less than 14 MPa. Although the ILSS value is higher than in previous studies, the still low ILSS value is considered to be a major obstacle to the application of cube satellites.

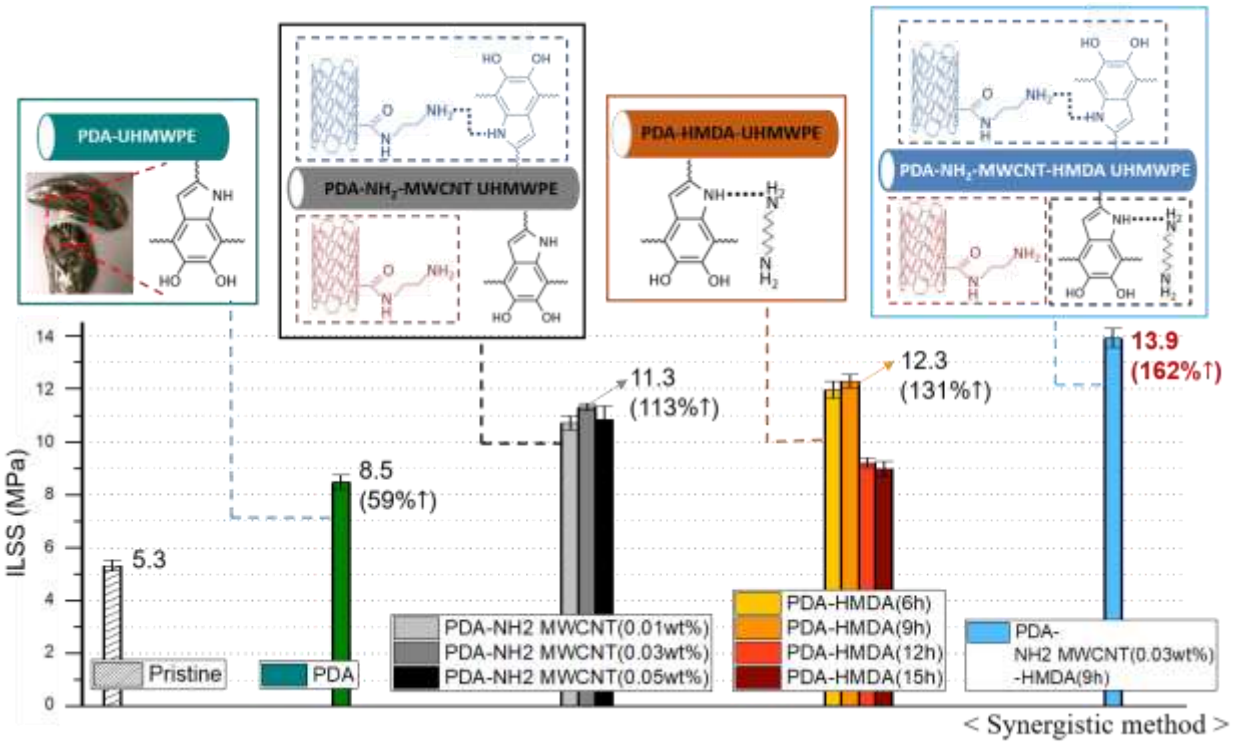

Figure 9 – ILSS according to fiber treatment and autoclave manufacturing process; Manufactured by curing at 130℃ for 7 hours in the final process.

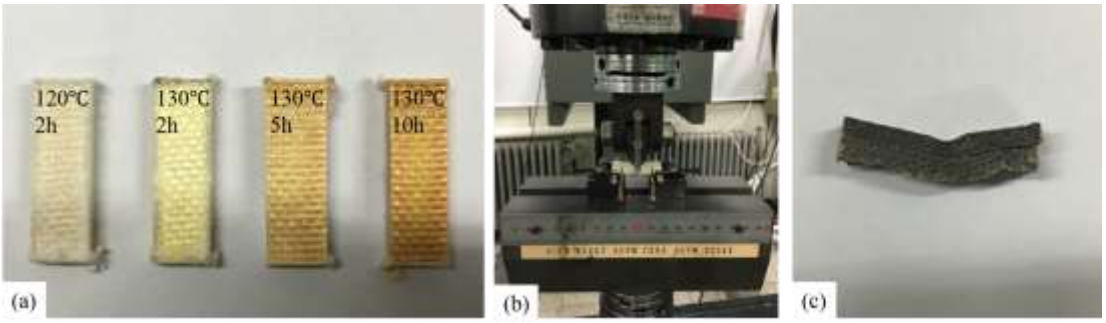

Figure 10 – (a) Specimens according to curing temperature and time; (b) ILSS test; (c) Specimens with interlaminar shear after testing.

4.4 Tensile strength

Fig. 11 shows the tensile test results of the UHC fabricated by the method proposed in this study. Since there is little difference in tensile strength performed in the previous study and this study, it can be judged that the specimen fabrication is sufficiently similar. Although the ILSS value was high in the heating process at 130°C for 10 h, it was confirmed that the tensile properties decreased in the tensile test. If high tensile properties are desired, a heating process of 130 degrees for 5 hours is recommended. The improved interfacial adhesion UHWMPE proposed in this study has about 20% higher tensile strength than the pristine UHMWPE. The coating-grafting method and curing conditions proposed in this study can increase not only the interlaminar shear strength but also the tensile properties.

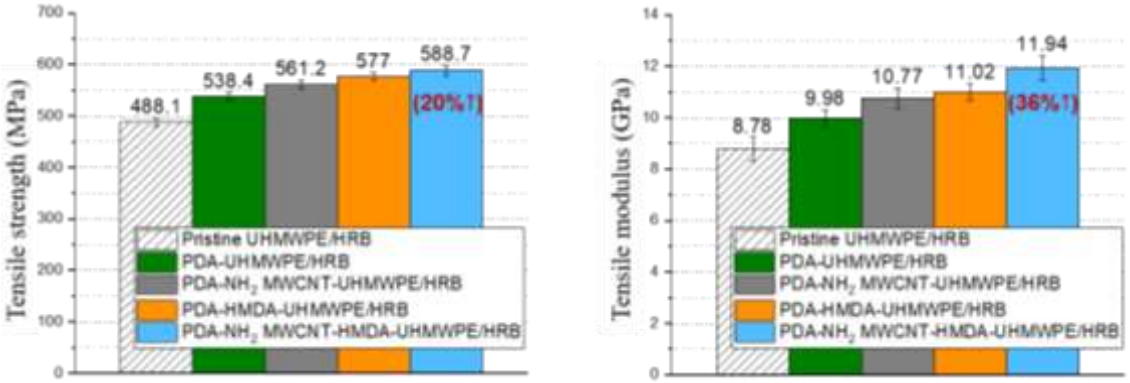

Figure 11 – Tensile property according to fiber treatment and autoclave manufacturing process; Manufactured by curing at 130℃ for 7 hours in the final process.

4.5 Modified fiber surface analysis

Table 3 shows the composition of UHMWPE surface components from XPS experiments. As in the previous study, nitrogen was detected in the dopamine coating, confirming the addition of amine groups. More amine groups can be added through additional grafted HMDA and NH2-MWCNT. Due to the addition of amine groups, the chemical bonding and curing of UHMWPE and HRB can be increased. In addition, MWCNTs grafted to the fibers act as physical anchors to strengthen the bonds between the fibers and the matrix, and the functionalized chemical groups facilitate dispersion in the HRB.

Table 5 – Surface element analysis of coated or grafted fibers via XPS

Coating and grafting	Composition			N/C
	C	O	N	
UHMWPE	96.78	3.22	-	0
PDA-UHMWPE	75.15	18.09	6.76	9.00%
PDA-HMDA-UHMWPE	74.61	16.83	8.56	11.47%
PDA-NH2 MWNCT-HMDA-UHMWPE	81.61	9.82	8.48	10.39%

4.6 Fourier-transform infrared spectroscopy analysis

FTIR analysis was performed to examine the differences in HRB according to the curing conditions, as shown in Fig. 12. To judge the degree of curing of HRB, six peaks mentioned in previous studies[10] were observed; 1) 966cm^{-1}: benzoxazine bonds (N–CH_2–O); 2) 1030 and 1156cm^{-1}: the aromatic ether of the benzene ring; 3) 1377cm^{-1}: the wagging of the hydrogen atoms in the fourth position; 4) 1500 and 1620cm^{-1}: trisubstituted benzene ring. It can be seen that the six peaks mentioned decreased under the curing condition of 130°C for 10 hours compared to the curing condition of 120°C for 2 hours, confirming that higher curing was achieved. These results suggest that there is a clear difference in the curing conditions of HRB.

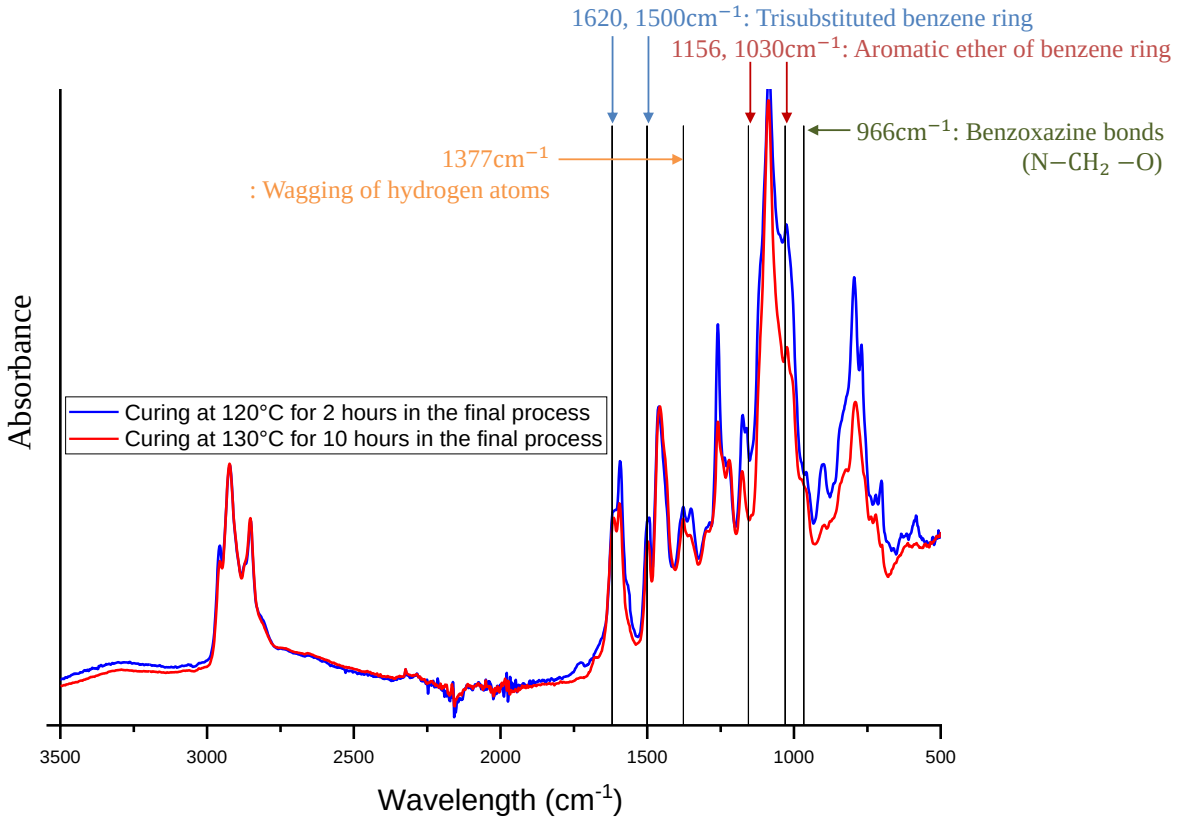

Figure 12 – FTIR analysis according to curing conditions of HRB.

4.7 Space environment resistance characteristics

The results of the outgassing test are shown in Table 6. The mean TMLs for UHC and PDA-UHMWPE/HRB were 0.2321% and 0.2263%, and the mean CVCM for UHC and PDA-UHMWPE/HRB were 0.0258% and 0.0212%, respectively. Since the general acceptance criteria for space application materials are TML <1.0 % and CVCM < 0.1 %, it has been confirmed that UHC and PDA-UHMWPE/HRB have excellent space environment resistance satisfying these conditions. The fibers are exposed in the cut cross section of the specimen, and it is presumed that the dopamine coating suppresses the outgassing of the UHMWPE, which improves the TML and CVCM performance. For comparison between UHC and PDA-UHMWPE/HRB, TML and CVCM tests of M55J/M18, a space-only CFRP, were performed. The CVCM performance of the PDA-UHMWPE/HRB was slightly lower, but the TML was excellent. From these results, it is judged that PDA-UHMWPE/HRB has as superior space environmental resistance as space-only materials.

Table 6 – Outgassing test results

	UHMWPE	UHC (Std. Dev.)	M55J/M18 CFRP (Std. Dev.)
TML (Std. Dev.)	1.38% [14]	0.2321% (0.0012)	0.3984% (0.0158)
CVCM (Std. Dev.)	0.072% [14]	0.0258% (0.0085)	0.0193% (0.0034)

5. Results and Discussion

To protect the satellite's COTS from cosmic radiation, the use of UHMWPE/HRB with improved interfacial adhesion has been proposed. Through elemental analysis of the manufactured HRB, it was confirmed that it was made identical to the theoretical composition. The dose analysis results calculated through OLTARIS proved that UHC and HRB have a dose reduction effect compared to existing space materials. To increase the interlaminar shear strength of UHC, dopamine coating, grafting of functionalized MWCNTs and HMDA was proposed, and the curing temperature and time were reviewed. By applying the methods proposed in this study, the ILSS could be improved by about 116% compared to the existing process, and the tensile strength could be improved by about 12%. Using XPS, the amine groups grafted to the fibers were identified. Using FTIR, the difference in HRB according to curing conditions was confirmed. In the outgassing test, it was confirmed that PDA-UHMWPE/HRB has very good TML and CVCM performance. The proposed material is expected to be utilized as a cosmic radiation shielding panel for future satellites.

Acknowledgments

The work was supported by the National Research Foundation of South Korea (NRF-2021R1A4A1032783). The authors would like to thank the foundation for the financial support received.

References

[1] Winokur PS, Lum GK, Shaneyfelt MR, Sexton FW, Hash GL, Scott L. Use of COTS microelectronics in radiation environments. IEEE Trans Nucl Sci 1999;46:1494–503. https://doi.org/10.1109/23.819113.

[2] Duzellier S. Radiation effects on electronic devices in space. Aerosp Sci Technol 2005;9:93–9. https://doi.org/10.1016/j.ast.2004.08.006.

[3] Donnell KO, Richardson G, Donnell O. Small Satellite Trending & Reliability 2009-2018. 34th Annu Small Satell Conf 2020.

[4] Sinclair D, Dyer J. Radiation Effects and COTS Parts in SmallSats. 27th Annu AIAA/USU Conf Small Satell 2013:1–12.

[5] National Aeronautics and Space Administration. Space Radiation Effects on Electronic Components in Low-Earth Orbit. Pract NO PD-ED-1258 1996:1–7.

[6] Barthel J, Sarigul-Klijn N. A review of radiation shielding needs and concepts for space voyages beyond Earth's magnetic influence. Prog Aerosp Sci 2019;110:100553. https://doi.org/10.1016/j.paerosci.2019.100553.

[7] Tsai PE, Heilbronn LH, Lai BL, Iwata Y, Murakami T, Sheu RJ. Thick target neutron yields from 100- and 230-MeV/nucleon helium ions bombarding water, PMMA, and iron. Nucl Instruments Methods Phys Res Sect B Beam Interact with Mater Atoms 2019;449:62–70. https://doi.org/10.1016/j.nimb.2019.04.030.

[8] European Space Agency, European Cooperation for Space Standarization. ECSS-E-HB-10-12A: Space Engineering Calculation of radiation and its effects and margin policy handbook 2010.

[9] Thibeault SA, Kang JH, Sauti G, Park C, Fay CC, King GC. Nanomaterials for radiation shielding. MRS Bull 2015;40:836–41. https://doi.org/10.1557/mrs.2015.225.

[10] Iguchi D, Ohashi S, Abarro GJE, Yin X, Winroth S, Scott C, et al. Development of Hydrogen-Rich Benzoxazine Resins with Low Polymerization Temperature for Space Radiation Shielding. ACS Omega 2018;3:11569–81. https://doi.org/10.1021/acsomega.8b01297.

[11] Winroth S, Scott C, Ishida H. Structure and performance of benzoxazine composites for space radiation shielding. Molecules 2020;25. https://doi.org/10.3390/molecules25184346.

[12] Ishida H, Allen DJ. Physical and mechanical characterization of near-zero shrinkage polybenzoxazines. J Polym Sci Part B Polym Phys 1996;34:1019–30. https://doi.org/10.1002/(SICI)1099-0488(19960430)34:6<1019::AID-POLB1>3.0.CO;2-T.

[13] Deitzel JM, McDaniel P, Gillespie JW. High performance polyethylene fibers. Elsevier Ltd; 2017. https://doi.org/10.1016/B978-0-08-100550-7.00007-3.

[14] Cha JH, Kim YH, Sathish Kumar SK, Choi C, Kim CG. Ultra-high-molecular-weight polyethylene as a hypervelocity impact shielding material for space structures. Acta Astronaut 2020;168:182–90. https://doi.org/10.1016/j.actaastro.2019.12.008.

[15] Sen S, Schofield E, O'Dell JS, Deka L, Pillay S. The development of a multifunctional composite material for use in human space exploration beyond low-earth orbit. Jom

2009;61:23–31. https://doi.org/10.1007/s11837-009-0019-5.

[16] Shanmugam L, Feng X, Yang J. Enhanced interphase between thermoplastic matrix and UHMWPE fiber sized with CNT-modified polydopamine coating. Compos Sci Technol 2019;174:212–20. https://doi.org/10.1016/j.compscitech.2019.03.001.

[17] Jin X, Wang W, Xiao C, Lin T, Bian L, Hauser P. Improvement of coating durability, interfacial adhesion and compressive strength of UHMWPE fiber/epoxy composites through plasma pre-treatment and polypyrrole coating. Compos Sci Technol 2016;128:169–75. https://doi.org/10.1016/j.compscitech.2016.03.026.

[18] Li W, Meng L, Ma R. Effect of surface treatment with potassium permanganate on ultra-high molecular weight polyethylene fiber reinforced natural rubber composites. Polym Test 2016;55:10–6. https://doi.org/10.1016/j.polymertesting.2016.08.006.

[19] Moon SI, Jang J. Effect of polybutadiene interlayer on interfacial adhesion and impact properties in oxygen-plasma-treated UHMPE fiber/epoxy composites. Compos Part A Appl Sci Manuf 1999;30:1039–44. https://doi.org/10.1016/S1359-835X(99)00022-6.

[20] Wang L, Gao S, Wang J, Wang W, Zhang L, Tian M. Surface modification of UHMWPE fibers by ozone treatment and UV grafting for adhesion improvement. J Adhes 2018;94:30–45. https://doi.org/10.1080/00218464.2016.1229603.

[21] Mohammadalipour M, Masoomi M, Ahmadi M, Safi S. Interfacial shear strength characterization of GMA-grafted UHMWPE fiber/epoxy/nano clay hybrid nanocomposite materials. RSC Adv 2016;6:41793–9. https://doi.org/10.1039/c6ra05027a.

[22] Mohammadalipour M, Masoomi M, Ahmadi M, Kazemi Z. The effect of simultaneous fiber surface treatment and matrix modification on mechanical properties of unidirectional ultra-high molecular weight polyethylene fiber/epoxy/nanoclay nanocomposites. J Compos Mater 2018;52:2961–72. https://doi.org/10.1177/0021998318755542.

[23] Chhetri S, Bougherara H. A comprehensive review on surface modification of UHMWPE fiber and interfacial properties. Compos Part A Appl Sci Manuf 2021;140:106146. https://doi.org/10.1016/j.compositesa.2020.106146.

[24] Smith A. Space engineering. Sp Sci 2004:443–58. https://doi.org/10.1142/9781860944574_0014.

[25] Brown EN, Willms RB, Gray GT, Rae PJ, Cady CM, Vecchio KS, et al. Influence of molecular conformation on the constitutive response of polyethylene: A comparison of HDPE, UHMWPE, and PEX. Exp Mech 2007;47:381–93. https://doi.org/10.1007/s11340-007-9045-9.

[26] Peijs T. High performance polyethylene fibers. Elsevier Ltd.; 2017. https://doi.org/10.1016/B978-0-12-803581-8.09876-3.

[27] Eakman D, Lambeck R, Mackowski M, Slifer L. Small Spacecraft Power Thermal Subsystems. NASA Contracor Rep 195029 1994.

[28] Son G, Kim CG. Protective effect of nanocomposite film from the low earth orbit environment. J Compos Mater 2015;49:2297–306. https://doi.org/10.1177/0021998314545189.

[29] Zeng S, Duan P, Shen M, Lu X, Xue Y, Yang L. Interlaminar fracture toughness, adhesion and mechanical properties of MWCNT–glass fiber fabric composites: Effect of MWCNT aspect ratios. Polym Compos 2019;40:E1329–37. https://doi.org/10.1002/pc.24990.

[30] Shanmugam L, Feng X, Yang J. Enhanced interphase between thermoplastic matrix and UHMWPE fiber sized with CNT-modified polydopamine coating. Compos Sci Technol 2019;174:212–20. https://doi.org/10.1016/j.compscitech.2019.03.001.

[31] Hu J, Feng X, Liu Z, Zhao Y, Chen L. Surface amine-functionalization of UHMWPE fiber by bio-inspired polydopamine and grafted hexamethylene diamine. Surf Interface Anal 2017;49:640–6. https://doi.org/10.1002/sia.6203.

[32] Lee W, Lee JU, Jung BM, Byun JH, Yi JW, Lee SB, et al. Simultaneous enhancement of mechanical, electrical and thermal properties of graphene oxide paper by embedding dopamine. Carbon N Y 2013;65:296–304. https://doi.org/10.1016/j.carbon.2013.08.029.

[33] Choi N, Park J. Fiber / matrix interfacial shear strength measured by a quasi-disk microbond specimen Pre-hole. Compos Sci Technol 2009;69:1615–22. https://doi.org/10.1016/j.compscitech.2009.03.012.

[34] Kartikeya K, Chouhan H, Ahmed A, Bhatnagar N. Determination of tensile strength of UHMWPE fiber-reinforced polymer composites. Polym Test 2020;82:106293. https://doi.org/10.1016/j.polymertesting.2019.106293.

[35] Singleterry RC, Blattnig SR, Clowdsley MS, Qualls GD, Sandridge CA, Simonsen LC, et al. OLTARIS: On-line tool for the assessment of radiation in space. Acta Astronaut

2011;68:1086–97. https://doi.org/10.1016/j.actaastro.2010.09.022.

[36] Wilson JW, Millar J, Konradi A, Cucinotta FA. Shielding Strategies for Human Space Exploration NASA Conference Publication 3360 Shielding Strategies for Human Space Exploration Edited by. Nasa Conf Publ 1997;3360.